Supramolecular Hydrogel Exhibiting Four Basic Logic Gate Functions To Fine-Tune Substance Release

ARTICLE *in* JOURNAL OF THE AMERICAN CHEMICAL SOCIETY · APRIL 2009

Impact Factor: 12.11 · DOI: 10.1021/ja8098239 · Source: PubMed

6 AUTHORS, INCLUDING:

Kenji Kaneko
Kyushu University
235 PUBLICATIONS **4,289** CITATIONS
SEE PROFILE

Masato Ikeda
Gifu University
77 PUBLICATIONS **3,026** CITATIONS
SEE PROFILE

JACS ARTICLES

Published on Web 03/30/2009

Supramolecular Hydrogel Exhibiting Four Basic Logic Gate Functions To Fine-Tune Substance Release

Harunobu Komatsu,[†] Shinji Matsumoto,[†] Shun-ichi Tamaru,[†] Kenji Kaneko,[‡] Masato Ikeda,[†] and Itaru Hamachi*[,†,§]

Department of Synthetic Chemistry and Biological Chemistry, Graduate School of Engineering, Kyoto University, Katsura, Kyoto 615-8510, Japan, Department of Materials Science & Engineering, Graduate School of Engineering, Kyushu University, Motooka 744, Nishi-ku, Fukuoka 819-0395, Japan, and Japan Science and Technology Agency (JST), CREST, Sanbancho 5, Chiyoda-ku, Tokyo 102-0075, Japan

Received December 29, 2008; E-mail: ihamachi@sbchem.kyoto-u.ac.jp

Abstract: Logic-gate operations displaying macroscopic outputs are promising systems for the development of intelligent soft materials that can perform effective functions in response to various input patterns. A supramolecular hydrogel comprising the phosphate-type hydrogelator **1** exhibits macroscopic gel−sol behavior in response to four distinct input stimuli: temperature, pH, Ca^{2+}, and light. We characterized this performance through microscopic, spectroscopic, and rheological measurements. On the basis of its multiple-stimulus responsiveness, we constructed gel-based supramolecular logic gates from hydrogelator **1** that demonstrated AND, OR, NAND, and NOR types of stimulus-responsive gel−sol behavior in the presence of various combinations of the four stimuli. Implementation of such logic-gate functions into semiwet soft materials (e.g., supramolecular hydrogels) is an important step toward the design of controlled drug delivery and release systems. Indeed, we demonstrate herein that one of our gel-based supramolecular logic gates is capable of holding and releasing bioactive substances in response to logic triggers. Furthermore, combining our supramolecular gel-based AND logic gate with a photoresponsive supramolecular gel could temporarily modulate the release rate of the bioactive substance.

Introduction

Following Aviram's and de Silva's pioneering investigations,[1] molecular logic gates have been actively studied with the goal of scaling down electrical and optical devices to the molecular level.[2] In addition to attempts to improve information processing, outputs manifested as effective functions controlled by particular inputs are now regarded as another potential path for the application of molecular logic gates.[3] When molecular logic gates are installed rationally, the resulting designer materials may become intelligent, i.e., exhibit macroscopic property changes that are induced in response to plural external stimuli.

One of the significant advantages of supramolecular materials is that appropriate design of small component molecules allows efficient control over the assembled structure and its function.[4] In some cases, a response on the molecular level can directly cause a physical or chemical change on the macroscopic level; such supramolecular logic gates can therefore perform effective functions depending on the input patterns. In this paper, we describe four fundamental logic gates displaying macroscopic outputs that can be installed in a single component of a supramolecular hydrogel. The new phosphate-type hydrogelator **1** exhibits a macroscopic gel−sol behavior in response to four

[†] Kyoto University.
[‡] Kyushu University.
[§] Japan Science and Technology Agency.

(1) (a) de Silva, P. A.; Gunaratne, N. H. Q.; McCoy, C. P. *Nature* **1993**, *364*, 42–44. (b) Aviram, A. *J. Am. Chem. Soc.* **1988**, *110*, 5687–5692.

(2) (a) Collier, C. P.; Wong, E. W.; Belohradský, M.; Raymo, F. M.; Stoddart, J. F.; Kuekes, P. J.; Williams, R. S.; Heath, J. R. *Science* **1999**, *285*, 391–394. (b) Raymo, F. M. *Adv. Mater.* **2002**, *14*, 401–414. (c) de Silva, A. P.; McClenaghan, N. D. *Chem.—Eur. J.* **2004**, *10*, 574–586. (d) Balzani, V.; Venturi, M.; Credi, A. *Molecular Devices and Machines: A Journey into the Nanoworld*; Wiley-VCH: Weinheim, Germany, 2003. (e) Pischel, U. *Angew. Chem., Int. Ed.* **2007**, *46*, 4026–4040. (f) Credi, A. *Angew. Chem., Int. Ed.* **2007**, *46*, 5472–5475. (g) de Silva, A. P.; Uchiyama, E. *Nat. Nanotechnol.* **2007**, *2*, 399–410, and references cited therein. In most of these studies, changes in fluorescence intensity are the outputs.

(3) Schneider et al. have reported macroscopic XOR or AND logic-gate responses of a polymer gel induced by chemical stimuli. See: (a) Schneider, H.-J.; Tianjun, L.; Lomadze, N.; Palm, B. *Adv. Mater.* **2004**, *16*, 613–615. For other examples of molecular logic-gate systems showing unique output responses, see: (b) Benenson, Y.; Gil, B.; Ben-Dor, U.; Adar, R.; Shapiro, E. *Nature* **2004**, *429*, 423–429. (c) Amir, R. J.; Popkov, M.; Lerner, R. A.; Barbas, C. F., III; Shabat, D. *Angew. Chem., Int. Ed.* **2005**, *44*, 4378–4381. (d) Muramatsu, S.; Kinbara, K.; Taguchi, H.; Ishii, N.; Aida, T. *J. Am. Chem. Soc.* **2006**, *128*, 3764–3769. (e) Baron, R.; Lioubashevski, O.; Katz, E.; Niazov, T.; Willner, I. *Angew. Chem., Int. Ed.* **2006**, *45*, 1572–1576. (f) de Silva, A. P.; James, M. R.; Mckinney, B. O. F.; Pears, D. A.; Weir, S. M. *Nat. Mater.* **2006**, *5*, 787–790. (g) Gianneschi, N. C.; Ghadiri, M. R. *Angew. Chem., Int. Ed.* **2007**, *46*, 3955–3958. (h) Rinaudo, K.; Bleris, L.; Maddamsetti, R.; Subramanian, S.; Weiss, R.; Benenson, Y. *Nat. Biotechnol.* **2007**, *25*, 795–801. (i) Win, M. N.; Smolke, C. D. *Science* **2008**, *322*, 456–460. (j) Ozlem, S.; Akkaya, E. U. *J. Am. Chem. Soc.* **2009**, *131*, 48–49.

(4) (a) Lehn, J.-M. *Supramolecular Chemistry: Concepts and Perspectives*; VCH: Weinheim, Germany, 1995. (b) *Supramolecular Polymers*, 2nd ed.; Ciferri, A., Ed.; Marcel Dekker: New York, 2000. (c) Brunsveld, L.; Folmer, B. J. B.; Meijer, E. W.; Sijbesma, R. P. *Chem. Rev.* **2001**, *101*, 4071–4098. (d) Special issue on supramolecular chemistry and self-assembly: *Science* **2002**, *295*, 2396−2421.

 10.1021/ja8098239 CCC: $40.75

distinct stimuli: temperature, pH, Ca^{2+}, and light. Taking advantage of these properties, we prepared AND, OR, NAND, and NOR types of stimulus-responsive semiwet materials that can hold and release bioactive substances selectively. Furthermore, a rational combination of our supramolecular gel-based AND logic gate with a photoresponsive supramolecular gel allowed us to further fine-tune the release function, e.g., the release rate of the bioactive substance could be temporarily modulated.

Results and Discussion

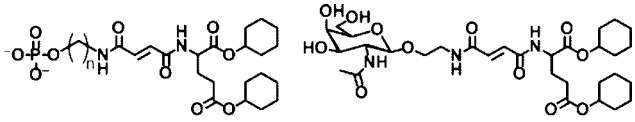

1: n = 8, **3**: n = 6, **4**: n = 4, **5**: n = 2 **2**

Molecular Design of Phosphate-Type Hydrogelators. We designed the phosphate-type hydrogelators **1** and **3**−**5** on the basis of a structural analysis of our previously established glycolipid-type hydrogelator, **2**.[5] We suspected that the amphiphilic structure of the phosphate-type hydrogelators would result in a heat-induced gel−sol transition similar to that of other small-molecule gelators.[5,6] In addition, we expected (i) the phosphate headgroup to potentially function as a moiety responsive to metal cations and/or protons (i.e., to pH changes) by changing the interfacial charge[7] and (ii) the olefinic bond incorporated into the spacer unit to alter the molecule's conformation between trans and cis under irradiation with light, thereby perturbing the molecular alignment of the gelator (Figure 1a).[8,9] These stimulus-sensitive modules could have positive or negative influences on the macroscopic gel−sol state (Figure 1b).[10] We prepared four phosphate-type hydrogelators with various alkyl chains (C_8H_{16} in **1**, C_6H_{12} in **3**, C_4H_8 in **4**, and C_2H_4 in **5**). It was found that **1** showed the lowest critical gelation concentration (CgC) (0.10 wt %) in the presence of Ca^{2+} (the values for **3** and **4** were 0.30 and 0.50 wt %, respectively, while **5** was insoluble). Thus, we used **1** to test the multiple-stimulus responsiveness in the following study.

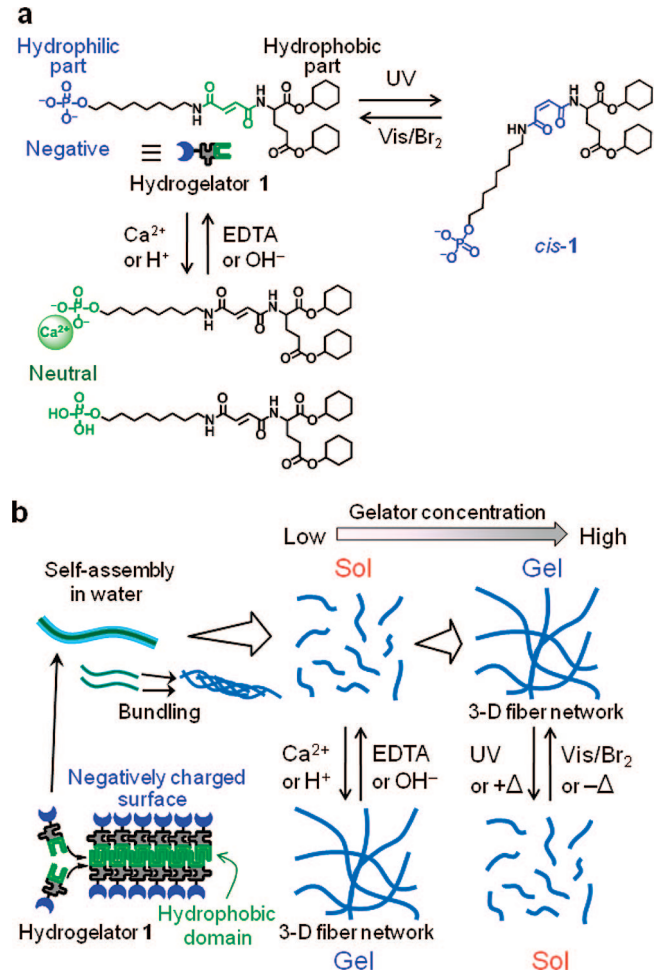

Figure 1. (a) Molecular structural changes in hydrogelator **1** in response to a variety of stimuli. (b) Schematic representation of the hierarchical molecular assembly of **1** to form a supramolecular hydrogel and its gel−sol transition triggered by four distinct stimuli (temperature, pH, Ca^{2+}, and light).

Multiple-Stimulus-Responsive Gel−Sol Transition of Hydrogelator 1. We initially examined the Ca^{2+} response of hydrogelator **1** by comparing the CgC's determined in the presence and the absence of Ca^{2+} (Figure 2a). It is clear that the CgC decreased from 1.0 to 0.10 wt % upon the addition of Ca^{2+}. On the other hand, the addition of EDTA, an effective chelator for Ca^{2+}, completely destroyed the hydrogel, indicating that the macroscopic gel−sol transition of **1** responds reversibly to the Ca^{2+} concentration (Figure 2b). The results of a rheological study (Figure 2c) were consistent with our macroscopic observations. For example, with 0.30 wt % **1** in the absence of Ca^{2+}, the values of the storage modulus G' and the loss modulus G'' were in almost the same range (~1 Pa), and both gradually decreased with decreasing rotational frequency. This behavior is typical of a viscous solution state but not a gel

(5) (a) Kiyonaka, S.; Sugiyasu, K.; Shinkai, S.; Hamachi, I. *J. Am. Chem. Soc.* **2002**, *124*, 10954–10955. (b) Kiyonaka, S.; Shinkai, S.; Hamachi, I. *Chem.—Eur. J.* **2003**, *9*, 976–983. (c) Kiyonaka, S.; Sada, K.; Yoshimura, I.; Shinkai, S.; Kato, N.; Hamachi, I. *Nat. Mater.* **2004**, *3*, 58–64. (d) Yoshimura, I.; Miyahara, Y.; Kasagi, N.; Yamane, H.; Ojida, A.; Hamachi, I. *J. Am. Chem. Soc.* **2004**, *126*, 12204–12205. (e) Yamaguchi, S.; Yoshimura, I.; Kohira, T.; Tamaru, S.-i.; Hamachi, I. *J. Am. Chem. Soc.* **2005**, *127*, 11835–11841. (f) Koshi, Y.; Nakata, E.; Yamane, H.; Hamachi, I. *J. Am. Chem. Soc.* **2006**, *128*, 10413–10422. (g) Wada, A.; Tamaru, S.-i.; Ikeda, M.; Hamachi, I. *J. Am. Chem. Soc.*, in press.

(6) (a) Estroff, L. A.; Hamilton, A. D. *Chem. Rev.* **2004**, *104*, 1201–1217. (b) de Loos, M.; Feringa, B. L.; van Esch, J. H. *Eur. J. Org. Chem.* **2005**, 3615–3631. (c) *Molecular Gels: Materials with Self-Assembled Fibrillar Networks*; Weiss, R. G., Terech, P., Eds.; Springer: Dordrecht, The Netherlands, 2006; Chapters 17 and 18. (d) Yang, Z.; Xu, B. *J. Mater. Chem.* **2007**, *17*, 2385–2393, and references cited therein.

(7) (a) Hartgerink, J. D.; Beniash, E.; Stupp, S. I. *Proc. Natl. Acad. Sci. U.S.A.* **2002**, *99*, 5133–5138. (b) Maitra, U.; Babu, P. *Steroids* **2003**, *68*, 459–463.

(8) (a) Matsumoto, S.; Yamaguchi, S.; Ueno, S.; Komatsu, H.; Ikeda, M.; Ishizuka, K.; Iko, Y.; Tabata, K. V.; Aoki, H.; Ito, S.; Noji, H.; Hamachi, I. *Chem.—Eur. J.* **2008**, *14*, 3977–3986. (b) Matsumoto, S.; Yamaguchi, S.; Wada, A.; Matsui, T.; Ikeda, M.; Hamachi, I. *Chem. Commun.* **2008**, 1545–1547.

(9) Frkanec, L.; Jokic, M.; Makarevic, J.; Wolsperger, K.; Zinic, M. *J. Am. Chem. Soc.* **2002**, *124*, 9716–9717.

(10) For stimulus-responsive supramolecular hydrogelators, see: (a) van Bommel, K. J. C.; van der Pol, C.; Muizebelt, I.; Friggeri, A.; Heeres, A.; Meetsma, A.; Feringa, B. L.; van Esch, J. *Angew. Chem., Int. Ed.* **2004**, *43*, 1663–1667. (b) Zhou, S.-L.; Matsumoto, S.; Tian, H.-D.; Yamane, H.; Ojida, A.; Kiyonaka, S.; Hamachi, I. *Chem.—Eur. J.* **2005**, *11*, 1130–1136. (c) Beck, J. B.; Rowan, S. J. *J. Am. Chem. Soc.* **2003**, *125*, 13922–13923. (d) Haines, L. A.; Rajagopal, K.; Ozbas, B.; Salick, D. A.; Pochan, D. J.; Schneider, J. P. *J. Am. Chem. Soc.* **2005**, *127*, 17025–17029. (e) Kim, H.-L.; Lee, J.-H.; Lee, M. *Angew. Chem., Int. Ed.* **2005**, *44*, 5810–5814. (f) Yang, Z.; Liang, G.; Wang, L.; Xu, B. *J. Am. Chem. Soc.* **2006**, *128*, 3038–3043.

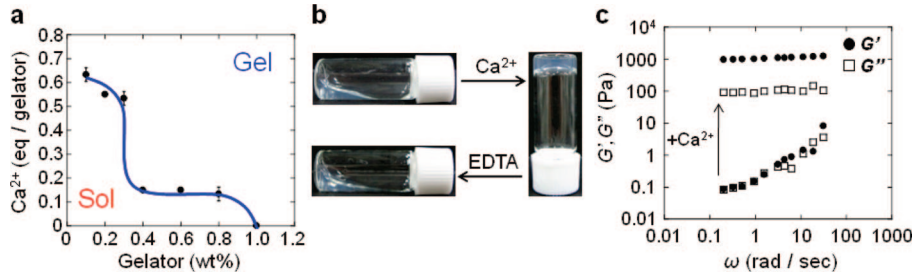

Figure 2. Ca^{2+} responsiveness of hydrogelator **1**. (a) Phase diagram of the gel−sol transition, revealing the number of equivalents of Ca^{2+} required to induce gelation at each gelator concentration. (b) Photographs of the Ca^{2+}-induced sol-to-gel transition ([**1**] = 0.30 wt %; $[Ca^{2+}]/[\mathbf{1}] = 1.0$; $[Na_2EDTA]/[Ca^{2+}] = 10$). (c) Corresponding dynamic viscoelastic properties before and after the addition of Ca^{2+}.

state. After the addition of Ca^{2+}, these values increased remarkably (by 200- and 1400-fold, respectively), with the value of G' being 10-fold greater than that of G'' over the entire range of rotational frequencies, indicative of a typical stable gel state. We also found that the subsequent addition of EDTA caused the values of G' and G'' to return to their original values (data not shown).

Confocal laser scanning microscopy (CLSM) images of the sol state stained with octadecylrhodamine B chloride (C_{18}-rhodamine) [Figure 3a and Figure S4a in the Supporting Information (a low-magnification image of Figure 3a)] and the histogram of the corresponding fiber length distribution (Figure 3b) revealed the presence of many short fibers less than 1 μm in length together with a few of long fibers possessing submicrometer diameters. On the other hand, in the Ca^{2+}-induced gel state [Figure 3c and Figure S4b in the Supporting Information (a low-magnification image of Figure 3c)], we observed a small number of short fibers less than 1 μm in length and a predominance of longer fibers, as shown in Figure 3d. In addition, gelation increased the number of cross-linking points from 30 (per 25 × 25 μm area in the sol) to 62 (per 25 × 25 μm area in the gel), suggesting that the long fibers more readily became entangled to form cross-linking points in the gel state. In the sol state, the short fibers rapidly fluctuated through Brownian motion because of the lack of efficient cross-linking (Figure S4a in the Supporting Information), while such fluctuating fibers were never observed in the Ca^{2+}-induced gel state (Figure S4b in the Supporting Information). Interestingly, from the real-time movie of the Ca^{2+}-induced sol-to-gel transition process, we noticed that short fibers were fused with other short fibers to form the longer ones (Figure S4c and Movie S1 in the Supporting Information). Transmission electron microscopy (TEM) images of the gel (Figure 3e) indicated long, thin (average width 30 nm) entangled fibers; energy dispersive X-ray (EDX) analysis traversing the fiber showed that peaks of C and P atoms due to gelator **1** overlapped well with the peak of the Ca atom (Figure 3f). Such coexistence of the gelator **1** with Ca in the fiber may be explained by Ca^{2+} complexes with phosphates, which are well-known to form one-dimensional polymeric structures in the crystalline state.[11] These lines of evidence suggested that neutralization of the self-assembled fibers and interphosphate coordination of the Ca^{2+} ions facilitated the longitudinal growth of the fibers, leading to a great enhancement of the degree of cross-linking essential for gelation.

Similar to its response to the addition of Ca^{2+}, neutralization of the anionic phosphate unit of the gelator **1** through acidification also induced the macroscopic phase transition. The viscous solution containing 0.30 wt % **1** became a stable hydrogel when

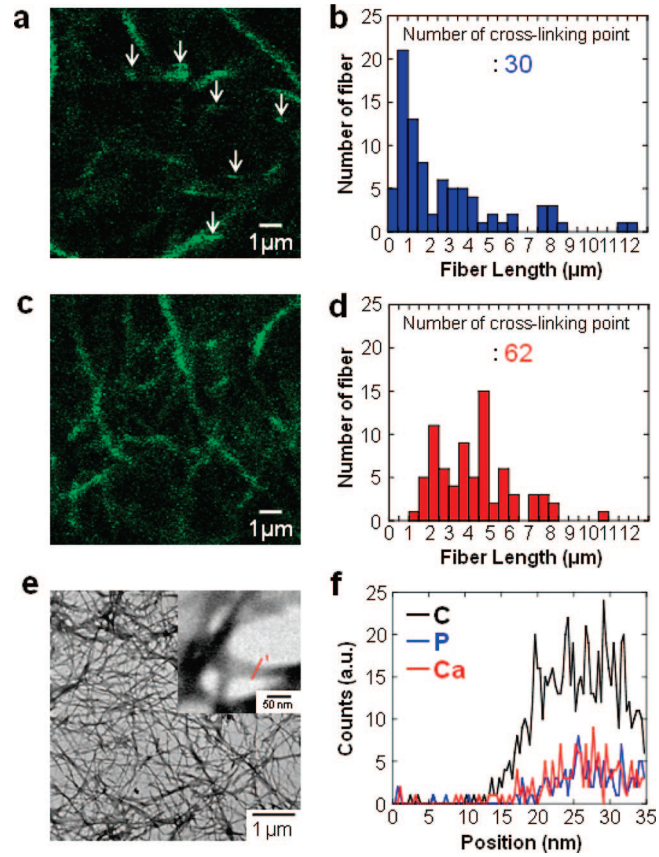

Figure 3. CLSM images of (a) sol **1** in the absence of Ca^{2+} and (c) hydrogel **1** in the presence of Ca^{2+} ([**1**] = 0.10 wt %; $[Ca^{2+}]/[\mathbf{1}] = 0.8$; [$C_{18}$-rhodamine] = 15 μM). The white arrows in (a) indicate short fibers less than 1 μm in length. The histograms of the fiber length distribution and the number of cross-linking points in (b) the sol state and (d) the gel state were obtained from the corresponding low-magnification CLSM images shown in Figure S4a,b in the Supporting Information. Since CLSM observations give two-dimensional images corresponding to a certain z-axis height of three-dimensionally entangled fibers in hydrogel, it was difficult to precisely evaluate the length of the longer fibers, unlike the short ones. (e) TEM image (inset: STEM mode, bright-field) of hydrogel **1** in the presence of Ca^{2+} ([**1**] = 0.30 wt %; $[Ca^{2+}]/[\mathbf{1}] = 0.80$). (f) EDX line profiles recorded along the red line displayed in the STEM image in the inset of (e).

the acidity was increased from pH 7.4 to 2.[12] The gel returned to the sol state when the the pH was increased to 8 through the addition of NH_3 (Figure S1 in the Supporting Information). Thus, it is clear that these two stimuli (Ca^{2+} and pH) operate as distinguishable inputs to produce a macroscopic output: the

(11) Bissinger, P.; Kumberger, O.; Schier, A. *Chem. Ber.* **1991**, *124*, 509–513.

(12) The pK_{a1} and pK_{a2} of the monomethyl ester of phosphoric acid were reported to be 1.5 and 6.3, respectively.[13]

(13) Kumler, W. D.; Eiler, J. J. *J. Am. Chem. Soc.* **1943**, *65*, 2355–2361.

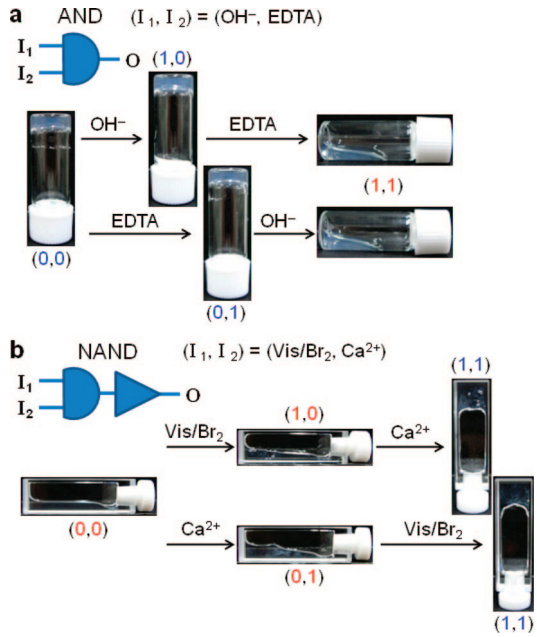

Figure 4. Gel-based supramolecular logic gates. (a) Photographs of the AND-type logic gate responses of hydrogel **1** ([**1**] = 0.30 wt %; $[Ca^{2+}]/[\mathbf{1}]$ = 0.60; pH 2) toward EDTA ($[Na_2EDTA]/[Ca^{2+}]$ = 3.0) and base (NH_3, pH 7−8) as input stimuli. (b) Photographs of the NAND-type logic gate responses of solution **1** (0.15 wt %; *cis*-**1** = ∼35%; pH 7.4) toward visible light and Ca^{2+} ($[Ca^{2+}]/[\mathbf{1}]$ = 1.0) as input stimuli.

gel−sol transition of the supramolecular hydrogel. The hydrogel of **1** also exhibited a photoresponsive gel-to-sol phase transition mediated by the photoinduced trans-to-cis conformational change of the olefinic unit in **1**.[8] A cis content of at least 13%, produced through irradiation with UV light, effectively destroyed the gel state ([**1**] = 1.0 wt %) to yield the viscous sol state, which returned to the gel under irradiation with visible light in the presence of a small amount of Br_2 (Figure S2 in the Supporting Information). Furthermore, the thermally induced gel-to-sol transition, akin to that of most other supramolecular hydrogels, occurred at 95 °C for a 1.0 wt % content of **1** (Figure S3 in the Supporting Information). These results indicate that four distinct stimuli (Ca^{2+}, pH, UV light, and temperature) can be used as effective inputs mediating the gel−sol transition of the hydrogel prepared from **1**.

Construction of Four Fundamental Logic Gates of Supramolecular Hydrogel 1. On the basis of its various response properties, we obtained an AND logic gate using the Ca^{2+}-complexed supramolecular hydrogel **1** at pH 2; this gate was operated through the addition of EDTA (i.e., decreasing the Ca^{2+} concentration) and NH_3 (i.e., a basic pH shift) as inputs (1) and (2), respectively. As indicated in Figure 4a, the gel state remained unaltered (output = 0) upon the addition of one input [either (1) or (2)], whereas the simultaneous addition of two inputs [both (1) and (2)] clearly altered the gel to the viscous sol (output = 1), regardless of the order of the inputs. Similarly, we constructed an OR logic gate comprising a high concentration of **1** at neutral pH, for which UV light and heat served as the two inputs. For this logic gate, it is clear that only one input was required to induce the gel-to-sol phase transition (Figure S5a in the Supporting Information). For our NAND and NOR logic gates, we employed visible light/Ca^{2+} and pH/Ca^{2+} stimulus pairs, respectively, as inputs. The sol-to-gel phase transition occurred in the NAND logic gate only in the presence of both visible light and Ca^{2+} (Figure 4b), whereas at least one

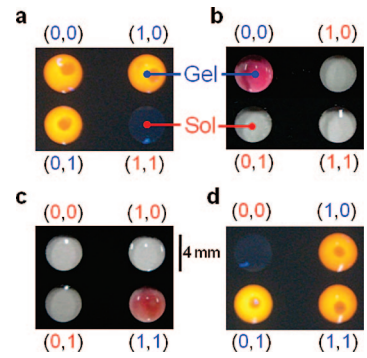

Figure 5. Photographs of hydrogel chips as holding matrices for bioactive substances [(a, d) Rh-ConA (0.5 mg/mL) under UV light at 365 nm; (b, c) vitamin B_{12} (0.5 mM) under white light] regulated by logic-gate processing: (a) AND-type gate (initial gel: [**1**] = 0.30 wt %; $[Ca^{2+}]/[\mathbf{1}]$ = 1.0; pH 2); (b) OR-type gate (initial gel: [**1**] = 1.0 wt %; pH 7.4); (c) NAND-type gate [initial sol: [**1**] = 0.15 wt % (*cis*-**1** = ∼35%); pH 7.4]. (d) NOR-type gate (initial sol: [**1**] = 0.30 wt %; pH 7.4).

input (pH or Ca^{2+}) was sufficient to cause the sol-to-gel change in the NOR logic gate (Figure S5b in the Supporting Information). In summary, we constructed four fundamental logic gates using the single-component gelator **1**.

Controlled Release of Bioactive Substances Performed by Gel-Based Supramolecular Logic Gates. Gels can hold a variety of substances in their networks, even when exposed to aqueous solutions.[14] We used the logic-gate processing described above to regulate the holding function of the gel formed from **1**. After mixing vitamin B_{12} or the protein Rh-Con A [rhodamine-labeled concanavalin A (a glucose-binding protein)] with the hydrogelator **1** arrayed on a glass plate, we applied the four types of inputs to the mixture spot and then dipped the processed plate into an aqueous buffer solution. Figure 5 displays a photograph of the gel array after dipping. In all cases, the substances were removed from the sol spots but remained in the gel spots. It is significant that the four distinct logic gates clearly conferred four different patterns in their behavior toward the holding substances. Thus, the input-dependent gel−sol transition can produce as an output a controlled release function, namely the holding and releasing of incorporated substances.

The supramolecular hydrogel can be used not only as the holding matrix but also as an intelligent barrier for the controlled release of biological substances. When we employed the AND logic gate as a barrier for vitamin B_{12} and bioactive proteins [fluorescein isothiocyanate (FITC)-insulin and FITC-bovine serum albumin (FITC-BSA)], the supramolecular logic gate executed a controlled release in response to the input patterns. After we covered the glycolipid-type of photoresponsive hydrogel (photogel) **2** containing vitamin B_{12} with a layer of the Ca^{2+}-complexed hydrogel **1** (the AND gel), we stimulated the composite hydrogel using two distinct inputs. As indicated in Figure 6a,b, no vitamin B_{12} was released within 3 h in the absence of the inputs or in the presence of only one input (i.e., the addition of either EDTA or NH_3). In contrast, when both inputs were applied simultaneously to the composite hydrogel, the AND gate hydrogel disappeared within 1 h because of the gel-to-sol phase transition, causing the gradual release of the vitamin B_{12} molecules embedded in the photogel below

(14) (a) Qiu, Y.; Park, K. *Adv. Drug Delivery Rev.* **2001**, *53*, 321–339. (b) Kikuchi, A.; Okano, T. *Adv. Drug Delivery Rev.* **2002**, *54*, 53–77. (c) Miyata, T.; Uragami, T.; Nakamae, K. *Adv. Drug Delivery Rev.* **2002**, *54*, 79–98, and references cited therein.

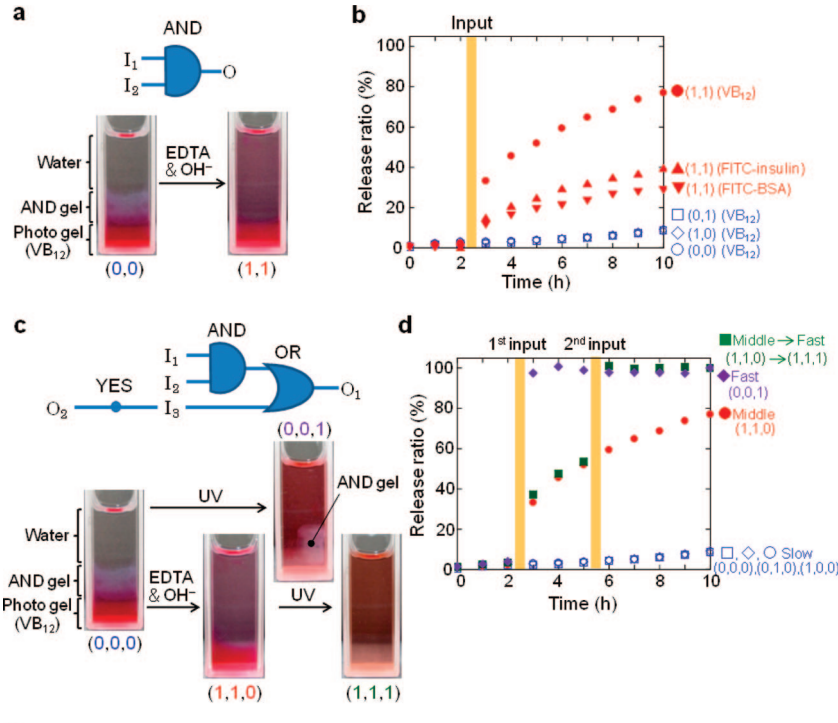

e

Input (I_1, I_2, I_3)			Output / 0 = Gel, 1 = Sol		
I_1 (EDTA)	I_2 (OH^-)	I_3 (UV)	O_1 (AND gel)	O_2 (Photo gel)	Release speed
0	0	0	0	0	Slow
0	1	0	0	0	Slow
1	0	0	0	0	Slow
1	1	0	1	0	Middle
0	0	1	1	1	Fast
0	1	1	1	1	Fast
1	0	1	1	1	Fast
1	1	1	1	1	Fast

Figure 6. Controlled release of bioactive substances by supramolecular hydrogel **1** (as a logic-gate barrier) and photogel **2** (as a holding matrix) and fine-tuning of the release function through a combination of AND logic gate operation and UV light stimulation. (a) Photographs displaying a supramolecular hydrogel gate composed of AND logic gate gel **1** and photogel **2** containing vitamin B_{12} in a 1 cm cell before and after the AND input; the logic scheme is also shown. (b) Corresponding time courses for the release of the bioactive substances (vitamin B_{12}, FITC-insulin, and FITC-BSA). (c) Photographs showing the supramolecular hydrogel gate holding vitamin B_{12} before and after application of UV light and the AND input and then after application of UV light subsequently; the combinatorial logic scheme is also shown. (d) Corresponding time courses of the vitamin B_{12} release. (e) Truth table for the combinational logic circuit.

the AND gate hydrogel. Similarly, we observed the AND-type release for insulin and BSA. In addition, we combined light-induced control with our AND release system to fine-tune the release function (Figure 6c,d). For example, when we irradiated the gel gate with UV light prior to applying the two AND inputs, we observed a more rapid release of vitamin B_{12}.[8a] On the other hand, when we applied the light input after the two AND inputs, the release rate of vitamin B_{12} was temporarily modulated. This is an example of the combination of AND and OR logic gates in these supramolecular hydrogel materials (Figure 6e).

Conclusion

We have used a single-component, multiple-stimulus-responsive hydrogelator **1** that displays a macroscopic gel−sol response toward four distinct input stimuli (temperature, pH, Ca^{2+}, and light) to construct gel-based supramolecular logic gates displaying AND, OR, NAND, and NOR functions. Using these logic gate functions, we developed gel-based supramolecular logic gates that were capable of holding and releasing bioactive substances in response to various input triggers. Combining our supramolecular gel-based AND logic gate with a photoresponsive supramolecular gel allowed us to further fine-tune the release function (e.g., the release rate of the bioactive substance could be temporarily modulated). The present results clearly indicate that the supramolecular approach is a powerful one for flexible installation of responses to various stimuli in soft materials. We believe that such intelligent supramolecular soft materials may have a variety of applications, such as within environment-sensitive actuators, cell cultures, and drug-delivery and controlled-release systems.

Experimental Section

General. Unless otherwise stated, all of the commercial reagents were used as received. FITC-insulin and FITC-BSA were purchased from Sigma. ^{1}H NMR spectra were obtained on a Varian Mercury 400 spectrometer with tetramethylsilane (TMS) or residual non-deuterated solvents as internal references. Fast-atom bombardment

Scheme 1. Synthesis of Hydrogelator **1**

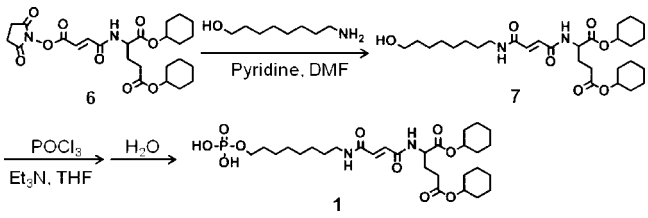

(FAB) high-resolution mass spectrometry (HRMS) was performed using a Shimadzu QP5050A instrument with glycerol as a matrix. Absorption spectra were measured using a Shimadzu UV-2550 spectrometer. Rheological measurements were carried out using a Reologica DynAlyser DAR-100 with a parallel plate (diameter = 4.0 cm) at a strain of 0.10% and a gap of 1.6 mm for frequency sweeps at 24 °C. Elemental analysis was carried out by the services at Kyoto University.

Syntheses. Compound **6** was synthesized according to the method reported previously by us.[8] The typical procedure for the synthesis of the phosphate-type hydrogelator **1** is shown in Scheme 1.

HO−(CH_2)$_8$−Fum−Glu−(O-cyclohexyl)$_2$ (7). To a solution of **6** (500 mg, 1.00 mmol) and 8-amino-1-octanol (178 mg, 1.16 mmol, 1.2 equiv) in dry DMF (10 mL) was added dry pyridine (3 mL), and the reaction mixture was stirred at room temperature for 8 h under an argon atmosphere. After removal of solvent, the resulting oil was dissolved in chloroform (100 mL) and washed with 0.1 M aqueous HCl (100 mL × 3). The organic layer was dried over anhydrous $MgSO_4$, and the solvent was evaporated to dryness. The resulting solid was washed with diisopropyl ether and dried in vacuo to afford **7** (332 mg, 0.618 mmol) in 63% yield as a white solid. ^{1}H NMR (400 MHz, $CDCl_3$, TMS, room temperature): δ 6.91 (d, J = 15 Hz, 1H, Fum-*H*), 6.87 (d, J = 15 Hz, 1H, Fum-*H*), 6.72 (br, 1H, N*H*), 5.85 (br, 1H, N*H*), 4.86−4.79 (m, 1H, OC*H*), 4.79−4.72 (m, 1H, OC*H*), 4.70−4.63 (m, 1H, NHC*H*), 3.64 (t, J = 6.8 Hz, 2H, (HOCH_2), 3.38−3.33 (m, 2H, CH_2NHCO), 2.46−2.28 (m, 2H, CH_2CO), 2.28−2.20 and 2.10−2.01 (m × 2, 1H × 2, CH_2CH$_2$CO), 1.88−1.20 (m, 32H, CH_2).

(HO)$_2$P(O)O−(CH_2)$_8$−Fum−Glu−(O-cyclohexyl)$_2$ (1). Under a nitrogen atmosphere, a solution of **7** (251 mg, 0.468 mmol) and triethylamine (0.194 mL, 1.40 mmol, 3.0 equiv) in dry THF (9 mL) was added dropwise to a solution of distilled phosphoryl chloride (0.45 mL, 4.68 mmol, 10 equiv) in dry THF (1 mL) on an ice bath with stirring over 1.5 h. After removal of the precipitate, ion-exchanged water was added to the filtrate, and the resultant suspension was extracted with chloroform (80 mL × 3). The organic layer was dried over anhydrous $MgSO_4$, and the solvent was evaporated to dryness. The obtained gel-like residue was washed with acetone, suspended in ion-exchanged water, and lyophilized to give hydrogelator **1** (144 mg, 0.234 mmol) in 50% yield as a white solid. ^{1}H NMR (400 MHz, CD_3OD, room temperature): δ 6.93 (d, J = 15.2 Hz, 1H, Fum-*H*), 6.90 (d, J = 15.2 Hz, 1H, Fum-*H*), 4.83−4.77 (m, 1H, OC*H*), 4.77−4.72 (m, 1H, OC*H*), 4.52−4.49 (m, 1H, NHC*H*), 3.98−3.93 (m, 2H, (HO)$_2$P(O)OCH_2), 3.29−3.26 (m, 2H, CH_2NHCO), 2.44−2.40 (m, 2H, CH_2CO), 2.24−2.17 and 2.03−1.95 (m × 2, 1H × 2, CH_2CH$_2$CO), 1.89−1.31 ppm (m, 32H, CH_2). HRMS (FAB, glycerol): m/z 617.3210 (calcd for $C_{29}H_{50}N_2O_{10}P$); m/z 617.3198 [M + H]$^+$). Anal. Calcd for $C_{29}H_{49}N_2O_{10}P$: C, 56.48; H, 8.01; N, 4.54. Found: C, 56.33; H, 8.24; N, 4.65.

CLSM Observations. A suspension of hydrogelator **1** (0.10 wt %, 1.6 mM) in 100 mM Tris-HCl buffer (pH 7.4) containing C_{18}-rhodamine (Molecular Probes) (15 μM) for staining gel fibers was heated to form a homogeneous solution. This solution (30 μL) was dropped to a glass-bottom Petri dish (Matsunami) and then observed with an inverted confocal laser scanning microscope (Olympus, FV1000, IX81) equipped with a 100×, NA = 1.40 oil objective and a 543 nm He−Ne laser by time-scan mode before and after the addition of 10 mM aqueous $CaCl_2$ solution (4.0 μL, 0.80 equiv/**1**). The obtained images were analyzed by software embedded in the apparatus.

TEM Observations. A suspension of hydrogelator **1** (0.10 wt %, 1.6 mM) in 100 mM Tris-HCl buffer (pH 7.4) was heated to form a homogeneous solution, and then 1.3 mM aqueous $CaCl_2$ solution (0.80 equiv/**1**) was added to the solution to form a gel. The gel (10 μL) was dropped on a copper TEM grid covered by an elastic carbon-support film (20−25 nm) and then dried under reduced pressure for at least 12 h. TEM observations were carried out using a JEOL JEM-1025 microscope (accelerating voltage 100 kV). STEM observations and EDS line-scan analyses were carried out using an FEI TECNAI-20 microscope (accelerating voltage 200 kV).

Photoisomerization. For trans-to-cis isomerization, the sample was irradiated with UV light in a quartz cell by a xenon lamp (500 W, Ushio Optical Modulex SX-UI500XQ) at 15 °C. For cis-to-trans isomerization, a sample containing a small amount of bromine was irradiated with visible light by the xenon lamp through two cutoff filters that blocked light with wavelengths of less than 300 and 350 nm. The photoisomerization ratios (trans/cis) were determined by ^{1}H NMR spectroscopic measurements after the samples were lyophilized and subsequently dissolved in CD_3OD.

Preparation of Controlled-Release Gel Systems. To a 1 cm quartz cell were added the bioactive substance (vitamin B_{12}, FITC-insulin, or FITC-BSA) and then the solution of hydrogelator **2** (600 μL, 0.10 wt % in ion-exchanged water) to form a photoresponsive hydrogel containing the bioactive substance. Above the hydrogel, the solution of hydrogelator **1** [600 μL, 0.20 wt % in 100 mM Tris-HCl buffer (pH 7.4)] was added, and then the mixture of 50 mM aqueous $CaCl_2$ solution (39 μL, 1.0 equiv/**1**) and 1.0 M aqueous HCl (25 μL) was added to form the AND-type logic gate gel. After ion-exchanged water (1.2 mL) was carefully added on top of the hydrogel, UV−vis absorption spectra of the upper-layer water were measured every 1 h to determine the release ratio. The two input stimuli were added after 2 and 5 h.

Final concentration of bioactive substances: [vitamin B_{12}] = 0.10 mM (detection wavelength = 550 nm), [FITC-insulin] = 15 μM (detection wavelength = 491 nm), [FITC-BSA] = 2.0 μM (detection wavelength = 491 nm).

Input stimuli: EDTA: 0.50 M, 58.4 μL (15 equiv/Ca^{2+}). NH_3: 1.0 M, 20 μL (until pH 8). UV light: xenon lamp (no filter), 40 min.

Acknowledgment. S.M. thanks JSPS for financial support through the Research Fellowship for Young Scientists. We thank Dr. K. Kuwata (Kyoto University) for HRMS measurements. We gratefully acknowledge financial support from the JST, the CREST program, the global COE program "Integrated Materials Science", and the Nanotechnology Network Program of the Ministry of Education, Culture, Science, Sports, and Technology (Japan).

Supporting Information Available: Figures showing the thermal, photo-, and pH responsiveness of hydrogelator **1**, time-lapsed CLSM images and a movie (AVI) recorded during the Ca^{2+}-induced sol-to-gel transition, and photographs of OR and NOR types of gel-based logic gates. This material is available free of charge via the Internet at http://pubs.acs.org.

JA8098239